

Thermohaline staircases in the Caribbean Sea

Otto Koetsier (4520335)

June 27, 2019

Supervisors: Dr. C.A. Katsman (TU Delft; chair), Prof. dr. J.D. Pietrzak (TU Delft), Ir. C.G. van der Boog (TU Delft) , Prof. dr. ir. H.A. Dijkstra (Utrecht University) and Prof. dr. L.R.M. Maas (Utrecht University)

Abstract

Thermohaline staircases are characterised by stepped vertical temperature, salinity and density profiles, which are formed and maintained by the double diffusion of heat and salt. Because double diffusion is the primary mixing agent in regions with staircases, it is the topic of extensive studies. Previous studies, however, are mainly theoretical and modelling orientated and observational evidence is needed to verify the results. In our study we use an extensive dataset with 460 vertical profiles of temperature and salinity. We found that staircases in the Caribbean Sea are related through temperature and salinity, indicating that staircases in the Caribbean Sea are constant in time and space. Individual steps, however, differ and were characterised in four types: well-developed steps, transitional layers, inversions and absence of steps. A case study of a strong anticyclonic eddy gave the indication that steps are influenced by short term processes. The eddy induces lateral gradients and hereby positions the water masses in the interior and exterior of the eddy such that thermohaline intrusions are initiated. The apparent preconditioning by the eddy, leading to thermohaline intrusions, allows us to speculate that the eddy is a catalyst in double diffusive diapycnal buoyancy transport.

1 Introduction

Thermohaline staircases are oceanographic structures which are characterised by stepped vertical temperature, salinity and density profiles (Radko, 2013) which indicates alternating homogeneous layers separated by thin high gradient interfaces. Staircases are formed and maintained by the double diffusion of heat and salt (Radko, 2013). Two regimes are known; the diffusive convection regime, where cold and fresh water overlies warm and salt water, and the salt finger regime, where warm and salt water overlies cold and fresh water. In this study we investigate the salt finger regime where fingerlike structures form due to the order of magnitude difference between the molecular diffusion rates of heat and salt (Radko, 2013). Downward moving fingers lose heat faster than salinity and thus increase in density, thereby increasing the initial movement. And vice

versa for upward moving fingers. Salt fingers thus lead to a nett downward diapycnal buoyancy transport (Radko, 2013).

The ratio of the background temperature and salinity gradients is expressed by the density ratio $R_\rho = \alpha T_z / \beta \bar{S}_z$ where \bar{T}_z and \bar{S}_z are respectively the background temperature and salinity gradients and α and β are respectively the thermal expansion and haline contraction coefficient. Salt finger staircases are observed when $1 < R_\rho < 2$ (St. Laurent and Schmitt, 1999) which implies that the stabilizing vertical temperature gradient should be approximately equal to, but not exceeding, the destabilizing vertical salinity gradient. In the Caribbean Sea staircases are located in Tropical Atlantic Central Water (TACW) which forms the interface between the warm and saline Subtropical Underwater (STUW) and the cold and fresh Antarctic Intermediate Water (AAIW) (van der Boog et al., 2019).

In regions with staircases, double diffusion is the dominant mixing agent (Radko, 2013). Staircases in the diffusive convection regime are found in high latitude regions and staircases in the salt finger regime are found in tropical regions. Most studies on salt finger staircases focus on the Tyrrhenean Sea (Zodiatis and Gasparini, 1996; Durante et al., 2019), the Mediterranean outflow (Ruddick and Hebert, 1988; Biescas et al., 2010) and the tropical North Atlantic, including the Caribbean Sea (Lambert and Sturges, 1977; Schmitt et al., 1987; Marmorino, 1991; Morell et al., 2006; Fer et al., 2010 van der Boog et al., 2019).

The most extensive survey near our study area is the C-SALT (Caribbean Sheets and Layers Transect) study which encompasses a large area in the tropical North Atlantic east of Barbados (Schmitt et al., 1987). Studies in the Caribbean Sea are less extensive. The study of Lambert and Sturges (1977) encompasses an area of $14 \times 10 \text{ km}$ at $17^\circ 40' N$, $65^\circ 20' W$ and presents measurements of only 4 days. In the study of Morell et al. (2006) only 8 vertical profiles are analysed and in the study of van der Boog et al. (2019) 15 vertical profiles are analysed. The generality with which staircases are observed indicates that staircases are a permanent feature in the Caribbean Sea. However, the sparseness of the data prevents making general conclusions.

Previous studies have investigated the influence of eddies on staircases (Ruddick and Hebert, 1988; Morell et al., 2006; Bebieva and Timmermans, 2016, 2017). Strong vertical velocity shear associated with the eddy azimuthal velocity may destroy staircases (Radko, 2013). However, Morell et al. (2006) found well developed staircases at the flanks of a cyclonic eddy in the Caribbean Sea implying that the azimuthal velocity was not strong enough to destroy staircases (Morell et al., 2006). The data from van der Boog et al. (2019) confirms this conclusion as the staircases in their study do not seem to be affected by an anticyclonic eddy.

Eddies also induce lateral gradients in temperature and salinity which may lead to thermohaline intrusions (overview in Ruddick and Richards, 2003a, b, Radko, 2013) observed as inversions in vertical temperature and salinity profiles (Marmorino, 1991; Morell et al., 2006; Bebieva and Timmermans, 2016). Intrusive diapycnal fluxes of heat and salt are furthermore found to result in a homogenization of water masses in the eddy edge resulting in a weakening of lateral gradients, which gives the strong indication that thermohaline intrusions increase eddy decay time scales (Ruddick and Hebert, 1988; Bebieva and Timmermans, 2016). Further observational evidence is however needed to verify the interaction of staircases with eddies (Ruddick and Richards, 2003a).

Our goals are to use our extensive dataset of 460 vertical temperature and salinity profiles to

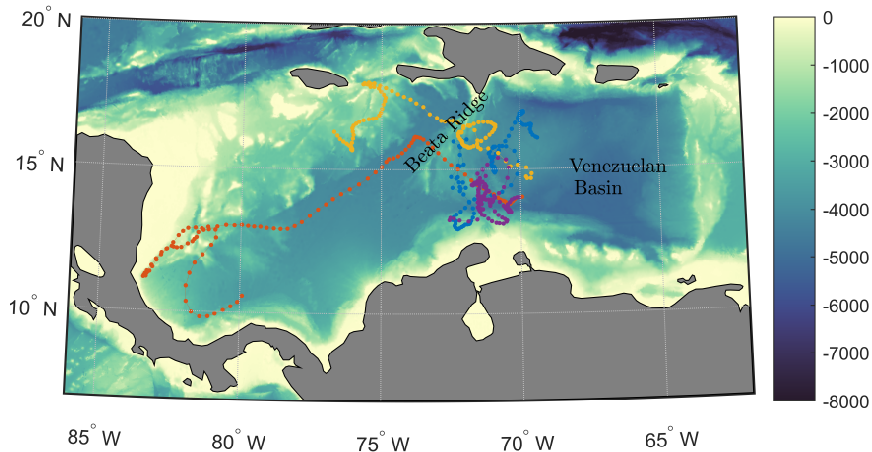


Figure 1: Bathymetry (m) and tracks of the four floats released during the NICO (Netherlands Initiative Changing Oceans) expedition (blue: float 3901985, orange: float 3901986, yellow: float 3901987, purple: float 3901979). Dots indicate profile locations, bathymetry data from General Bathymetric Chart of the Oceans (<https://www.gebco.net>). Colourmap from Thyng et al. (2016).

provide a general overview of staircase characteristics in the Caribbean Sea and to investigate the interaction of staircases with an anticyclonic eddy. In Chapter 2 the data and data processing is discussed. To provide a general overview of staircases in the Caribbean Sea (Chapter 3) we subdivided the steps in four types: I *well-developed steps*, II *inversions*, III *transitional layers* and IV *absence of steps*. We also found that staircases in the Caribbean Sea are related by their temperature and salinity. The investigation in staircase characteristics indicated that staircase variation is likely determined by short term processes. We observed a strong variation in types and temperature and salinity of steps coinciding with an anticyclonic eddy which motivated us to conducted a case study (Chapter 4) in which we investigated staircase characteristics under a strong anticyclonic eddy. In Chapter 5 we summarise and discuss the results.

2 Data and Methodology

In this chapter we introduce our data. We first introduce the data sources (section 2.1) after which we discuss how to interpret the data (section 2.2.). In section 2.3 we introduce an algorithm that is used for the automated detection of steps. In section 2.4 we discuss how we calculated the density ratio.

In the following sections we will refer to thermohaline staircases as *staircases*, being a sequence of *homogeneous layers* interchanged by high gradient interfaces. We will refer to high gradient interfaces as *interfaces*. A *step* or *layer* is defined as a homogeneous layer and its above interface.

2.1 Data sources

In this research we use data from four Argo floats released during the expedition of the Netherlands Initiative Changing Oceans (NICO) expedition (van der Boog et al., 2019). In total 460 vertical profiles of temperature and salinity were measured in the period from 6/Feb/2018 till 13/Jan/2019 by the four floats (Fig. 1). During this period two floats stayed in the Venezuelan Basin (blue and purple in Fig. 1) and two floats crossed the Beata Ridge (yellow and orange in Fig. 1). All floats have a parking depth at 500 *dbar* and a cycling period of three days. Data is converted to Conservative Temperature (T) and Absolute Salinity (S) with the TEOS-10 Matlab tool (McDougall and Barker, 2011).

Sea level anomaly (SLA) and geostrophic velocities (u, v) were downloaded from the Copernicus Marine Environment Monitoring Service (CMEMS; <http://marine.copernicus.eu>) and subsequently coupled to the location of vertical profiles for further analysis.

2.2 Vertical profile interpretation: Lagrangian versus Eulerian

Staircases in the present study are found in the depth range 300–600 *dbar*. The Argo float parking depth is at 500 *dbar* and floats are thus for the majority of the time (67-70 hours) advected with the staircases. Mean velocities in layers below 300 *dbar* are however in the order of 0.05 *m/s* (Gordon, 1967) and Argo floats in the present study spend 2 to 5 hours at the surface, which may affect the float position significantly because the mean surface velocity is approximately 0.2 *m/s* (CMEMS) and thus an order of magnitude larger than the deep water velocities. If the float advection at parking depth is significantly larger than the float advection at the surface, the data would give a Lagrangian view of staircase evolution. But if the float advection at the surface has the same order of magnitude as the float advection at parking depth the data should be interpreted as Eulerian.

The Argo floats in the present study are programmed as follows. The Argo float cycle starts with a descent to parking depth ($d_P = 500$ *dbar*). The time and date of the start of the descent are referred to as *Descent Start* (DST) and the time and date of the end of the descent are referred to as *Parking Start* (PST). The float is then advected at parking depth until a further descent (maximum depth stored as d_D) and a subsequent ascent of which time and date stored as *Ascent Start* (AST) and at which vertical profiles of temperature and salinity are taken with an interval of 1 *dbar*. The end time and date of the ascent are stored as *Ascent End* (AET). At the surface the float makes contact with a satellite to transmit the data. After transmitting the float descends again.

To estimate surface advection ($dX_{surface}$ in longitudinal and $dY_{surface}$ in latitudinal direction) we use the following expressions:

$$dX_{surface,i} = a \frac{d_L}{d_P} (PST_i - DST_i) u_{i-1} + a \frac{d_L}{d_D} (AET_i - AST_i) u_i + (DST_{i+1} - AET_i) u_i \quad (1)$$

$$dY_{surface,i} = a \frac{d_L}{d_P} (PST_i - DST_i) v_{i-1} + a \frac{d_L}{d_D} (AET_i - AST_i) v_i + (DST_{i+1} - AET_i) v_i \quad (2)$$

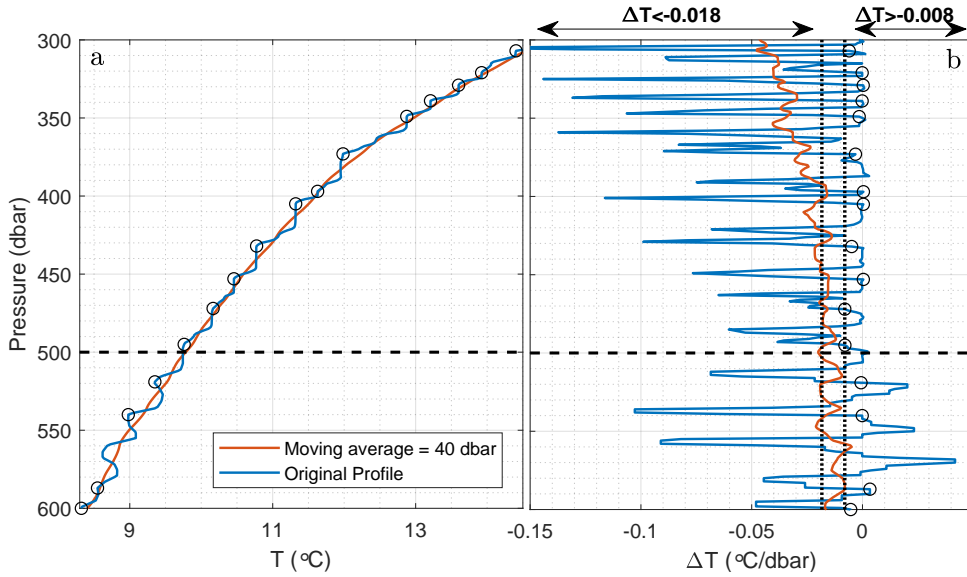


Figure 2: (a) Vertical Conservative Temperature ($^{\circ}\text{C}$) profile and (b) gradient of Conservative Temperature ($^{\circ}\text{C}/\text{dbar}$) (blue line) and (a,b) the corresponding vertical background profiles obtained with a moving average of 40 *dbar* (orange lines). Black circles indicate the top of an automatically detected homogeneous layer, the horizontal dashed line indicates the Argo float parking depth. (b) Vertical dotted lines at $\Delta T = -0.008^{\circ}\text{C}/\text{dbar}$ and $\Delta T = -0.018^{\circ}\text{C}/\text{dbar}$ indicate boundaries of the range given by the arrows on the top of the plot, as used for step detection.

With a being a factor determining the influence of surface velocity, d_L the depth of surface velocity influence, u and v respectively the longitudinal and latitudinal component of the geostrophic velocity (CMEMS) at the float's location and subscript i indicates the float cycle. The surface advection from expressions in (1) and (2) thus consist of three periods; the descent up to 200 *dbar*, the ascent from 200 *dbar* to the surface and the period from the end of the ascent to the subsequent descent.

In the study of van der Boog et al. (2019) strong velocities were observed above 200 *dbar*. This motivated us to define surface advection as advection of the upper 200 *dbar* layer ($d_L = 200$ *dbar*). We furthermore assume a linear decrease of the velocity from the surface to d_L , giving $a = 0.5$. We found the surface advection to be $2.7 \text{ km} \pm 1.4 \text{ km}$ (mean and standard deviation) which is in the order of 10 – 20 % of the total float advection. Increasing the surface velocity influence by setting $a = 1$ shifts the surface advection to 20% of the total advection. The estimates are rough, but give the strong indication that surface advection cannot be neglected and that the vertical temperature and salinity profiles should be interpreted as Eulerian or at least semi-Lagrangian.

2.3 Step detection

For further analysis we therefore developed an algorithm to automatically detect steps and inversions in the vertical temperature and salinity profiles. We based the algorithm on vertical

temperature profiles (blue line in Fig. 2a). Manually identified steps were compared with automatic detected steps and we found most agreement (not quantified) with the following criteria:

$$\frac{1}{3} \left(\left[\frac{\Delta T}{\Delta z} \right]_i + \left[\frac{\Delta T}{\Delta z} \right]_{i-1} + \left[\frac{\Delta T}{\Delta z} \right]_{i-2} \right) < -0.018 \text{ } ^\circ\text{C}/\text{dbar} \quad (3)$$

$$\left[\frac{\Delta T}{\Delta z} \right]_{i+2}, \left[\frac{\Delta T}{\Delta z} \right]_{i+3}, \left[\frac{\Delta T}{\Delta z} \right]_{i+4} > -0.008 \text{ } ^\circ\text{C}/\text{dbar} \quad (4)$$

In which $\Delta T/\Delta z$ is the Conservative Temperature gradient ($^\circ\text{C}/\text{dbar}$) calculated per measurement taken with an interval of 1 *dbar* (blue line in Fig. 2b), i indicates the top of a homogeneous layer (black circles in Fig. 2).

The criterium in expression 3 is set to ensure that the mean vertical temperature gradient of the high gradient interface is larger in absolute value than $-0.018^\circ\text{C}/\text{dbar}$ (see arrows on top of Fig. 2b). A mean value is used to average out small irregularities in the interface and to include steps with a relatively smooth transition in vertical temperature gradients from high gradient interface to homogeneous layer (note that the transition in vertical temperature gradient of the interface to the homogeneous layer of the temperature inversion at 570 *dbar* in Figure 2 is too smooth and therefore not identified as a step).

The criterium in expression 4 is set to ensure that the vertical temperature gradient of the homogeneous layer is smaller in absolute value than $-0.008^\circ\text{C}/\text{dbar}$ or positive (see arrows on top of Fig. 2b). Positive gradients in temperature imply inversions in the vertical temperature profile which we want to take into account in our analysis. By using the gradient up to $i + 4$ we ensure a homogeneous layer thickness of at least 4 *bar* which, in combination with the criterium for the minimal size of the interface thickness, was found to be an appropriate condition for a minimal step size. We use a minimal step size to prevent the identification of small regularities as steps.

Manual inspections showed staircases only in the 300 – 600 *dbar* depth range. The upper 100 *dbar* of the vertical temperature profile was excluded from the analysis as high vertical temperature gradients result in unwanted step detection.

Some steps were not recognized by the algorithm (not quantified), as for example the step at 365 *dbar* in Figure 2 and some structures were wrongly identified as steps (not quantified). We used the data for a statistical analysis and therefore chose to not manually correct the results of the algorithm.

2.4 Calculation method of the density ratio

In the introduction we defined the density ratio $R_\rho = \alpha \bar{T}_z / \beta \bar{S}_z$, in which \bar{T}_z and \bar{S}_z are respectively the background vertical temperature and salinity gradients and α and β are respectively the thermal expansion and haline contraction coefficients (Bebieva and Timmermans, 2016). Salt finger staircases are found only if $1 < R_\rho < 2$ (St. Laurent and Schmitt, 1999). In our study, background gradients were obtained by a vertical moving average of the original vertical profiles of temperature and salinity. For a moving average lower than 30 *dbar* we found a large variation

in the density ratio as one would expect because of the strong gradients in the original vertical temperature and salinity profiles. A too high value for the moving average, on the other hand, results in averaging out all variability. We found a convergence of the variance at a moving average higher than 30 *dbar*. For further analysis we chose a slightly higher value of 40 *dbar* to be sure in averaging out all steps. The resulting background temperature profile is shown as the orange line in Figure 2a.

3 Characteristics of staircases in the Caribbean Sea

To provide an overview of staircase characteristics in the Caribbean Sea we subdivided the vertical temperature profiles into four types (section 3.1). We furthermore investigated the temperature and salinity of staircases which we found to be very consistent in time and space (section 3.2).

3.1 Step subdivision in types

A manual investigation of vertical temperature profiles allowed us to subdivide the steps into four types which are also found in observational studies (Morell et al., 2006; Bebieva and Timmermans, 2016; Durante et al., 2019); (I) *well-developed steps*, (II) *inversions*, (III) *transitional layers* and (IV) *absence of steps* (Fig. 3).

(I) Well-developed steps are characterised by a combination of an interface with a vertical temperature gradient in the order of $-0.08^{\circ}C/dbar$ and a homogeneous layer with a negligible vertical temperature gradient. Well-developed step heights are in the order of 5 – 20 *dbar*. (II) Inversions are characterised by a sequence of negative and positive vertical temperature gradients. Inversions can be in the order of 2 *dbar* (lower arrow in Fig. 3b), but inversions in the order 40 *dbar* are also observed (upper arrow and circle in Fig. 3b). (III) Transitional layers (circled in Fig. 3d) are characterised as small steps (order 2 – 5 *dbar*) positioned in between two significantly larger steps. Vertical temperature gradients of the interface and homogeneous layer of transitional layers are similar to the gradients of the interface and homogeneous layer of well-developed steps. (IV) An absence of steps (Fig. 3d) is characterised by a profile with small irregularities which are not identified as steps by the algorithm discussed in section 2.3.

Manual investigation showed that vertical temperature profiles often contain more step types which hampers quantitative conclusions on the extent of step types over the area. However, 29% of the profiles has less or equal than 4 well-defined steps and is largely of type IV (Fig. 3d). 71% has more than 4 well-defined steps and is of type I (Fig. 3a). We furthermore found no spatial or temporal pattern in the occurrence of types which gives the strong indication that short term processes are important in the evolution of staircases in the Caribbean Sea.

Salt finger staircases are observed for a density ratio in the range $1 < R_{\rho} < 2$ (St. Laurent and Schmitt, 1999). Values of the density ratio in the study are represented as grey dots in Figure 4 which shows that in the depth range 300 – 550 *dbar* the density ratio is always in the $1 < R_{\rho} < 2$ range (indicated by black dotted vertical lines in Fig. 4). In an absence of any destructive process, well-developed steps (Fig. 3a) are thus expected in all vertical profiles (St. Laurent and Schmitt,

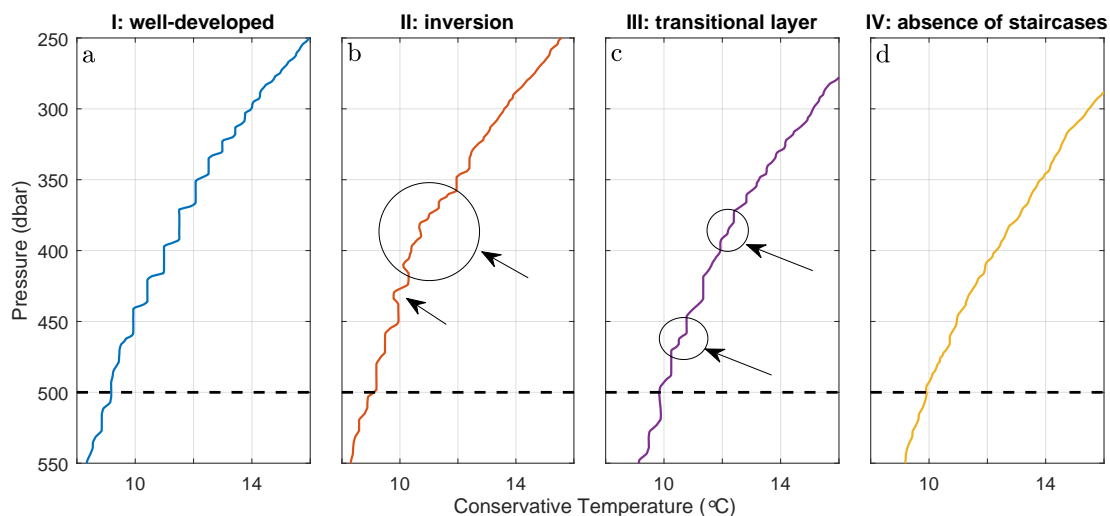


Figure 3: Vertical temperature profiles with examples of four observed step types and horizontal dashed line representing the Argo float parking depth. (a) I: well-developed steps, (b) II: inversions, the upper arrow indicates a large inversion, the lower arrow indicates a small inversion, (c) III: transitional layers, the upper arrow indicates a transitional layer with less defined interfaces, the lower arrow indicates a transitional layer with well defined interfaces and (d) IV: absence of steps (see text for explanation of the types).

1999; Radko, 2013) and other types (Fig. 3b-d) provide valuable information on processes affecting the staircases.

The density ratio may be inversely proportional to the step height (Radko, 2003; Radko, 2005), which is substantiated by a comparison of steps in the Tyrrhenian Sea and steps observed in our data: the density ratio in the Tyrrhenian Sea is with a mean value of $R_\rho = 1.25$ (Durante et al., 2019) significantly lower than the mean density ratio in this study of $R_\rho = 1.7$ (300 – 550 dbar). Step heights in the Tyrrhenian Sea are in the order of 100 dbar while step heights in our study are in the order of 15 dbar. The tendency of smaller steps at the top and bottom of staircases (Fig. 3a) may provide further evidence for this inverse proportionality as the density ratio follows a parabolic depth profile (grey dots Fig. 4).

Merryfield (2000) theoretically derived that thermohaline intrusions may equilibrate in steps if the density ratio is below a critical value ($R_{\rho,critical} \approx 1.7$). Thermohaline intrusions form in the presence of lateral temperature and salinity gradients (overview in Ruddick and Richards, 2003a, b; Radko, 2013; in section 4.4 the formation mechanism is explained). For higher density ratios thermohaline intrusions equilibrate as inversions (Merryfield, 2000). Morell et al. (2006) found statistical evidence for the theory of Merryfield (2000) by comparing the density ratio at observations of inversions with the density ratio at observations of well-defined steps. They however based their conclusion on 'only' 27 steps and 13 inversions. By using the same approach as Morell et al. (2006) we found no statistical evidence for the theory of Merryfield (2000). We furthermore note that the density ratio is obtained from stepped profiles and the density ratio

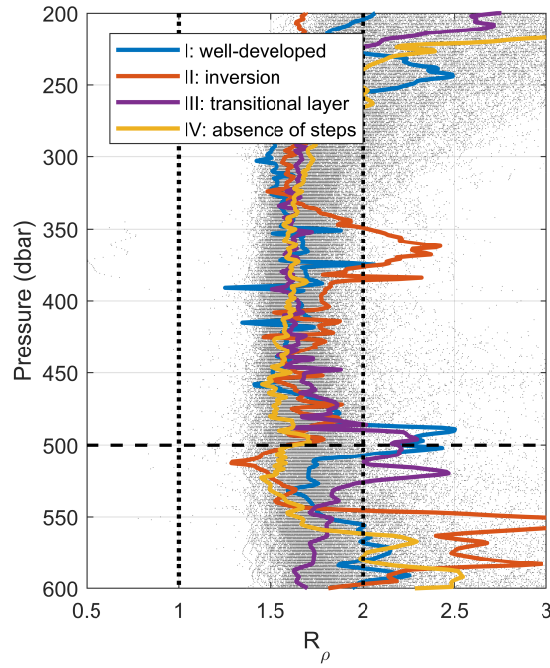


Figure 4: Density ratio ($R_\rho = \alpha \bar{T}_z / \beta \bar{S}_z$) in depth range 200 – 600 *dbar*, grey dots indicate all calculated values, coloured lines match the types as shown in Figure 3; I: well-developed steps (blue), II: inversions (orange), III: transitional layers (purple) and IV: absence of steps (yellow), vertical dotted lines indicate the range $1 < R_\rho < 2$ in which staircases are generally observed.

is thus sensitive to the used averaging method (see section 2.3). In this study we use a moving average of 40 *dbar* and the calculated density ratio is thus affected by intrusions of the same order of magnitude, as shown at 350 – 390 *dbar* in Figure 4 and 3b (orange line).

Transitional layers (Fig. 3c) are characterised as relatively small steps (2 – 5 *dbar*) in between two regular sized steps (15 *dbar*). The formation mechanism has not yet been resolved (Radko, 2013). A study of Marmorino (1989) investigated the role of vertical shear induced Kelvin-Helmholtz waves in the formation of transitional layers but could find no observational evidence. Transitional layers in our data are observed in vertical temperature profiles with a relatively large interface thickness (for example the interface at 430 – 445 *dbar* in Fig. 3c) which gives the indication that transitional layers form due to the splitting of an interface. A large interface thickness indicates the presence of turbulence (Radko, 2013) which gives the indication that transitional layers represent a metastable state in an environment of increased turbulence, and possibly increased vertical shear, pointing towards a role of Kelvin-Helmholtz waves (Marmorino, 1989) in the formation of transitional layers.

The absence of steps (Fig. 3d) in vertical temperature profiles in this study is not related to a disturbed density ratio because the density ratio in the study area is almost always in the range where steps are observed (range indicated by black dotted lines in Fig. 4). The yellow line in Figure 4 for example corresponds to a profile with an absence of steps. Increased turbulence in the staircase layer may destroy steps (Radko, 2013) when turbulent mixing is stronger than salt finger mixing (Radko, 2013). A vertical temperature profile with an absence of steps may also indicate a lack of formation. In the previously discussed theory of Merryfield (2000) lateral gradients are necessary for step formation. Morell et al. (2006) observed less developed steps under an eddy core where turbulence is generally low and lateral temperature and salinity gradients are weak. In section 4.3 and 4.4 we investigate the possible effect of lateral gradients and turbulence on the staircases.

3.2 Temperature and salinity of staircase in the Caribbean Sea

Dots in Figure 5 represent the temperature and salinity of all homogeneous layers detected by our algorithm (section 2.3). The majority of dots is arranged on distinct lines which indicates that the majority of staircase in the study area is related through temperature and salinity. A comparison of Figure 5 with the C-SALT staircases (Schmitt et al., 1987) shows that C-SALT staircase also fall on the lines of Figure 5. The C-SALT study is conducted in 1985 east of Barbados. The relation between temperature and salinity of the staircase in the present research and the C-SALT study thus gives the strong indication that staircase in the Caribbean Sea and North Atlantic Ocean are constant in time and space.

The gradient of the lines in Figure 5 is found to be related to the ratio of the heat flux (F_T) and the salt flux (F_S ; Radko, 2013):

$$\gamma = \frac{\alpha F_T}{\beta F_S} \quad (5)$$

We found a flux ratio of $\gamma = 0.79 \pm 0.04$. $\gamma < 1$, and the salt flux thus exceeds the heat

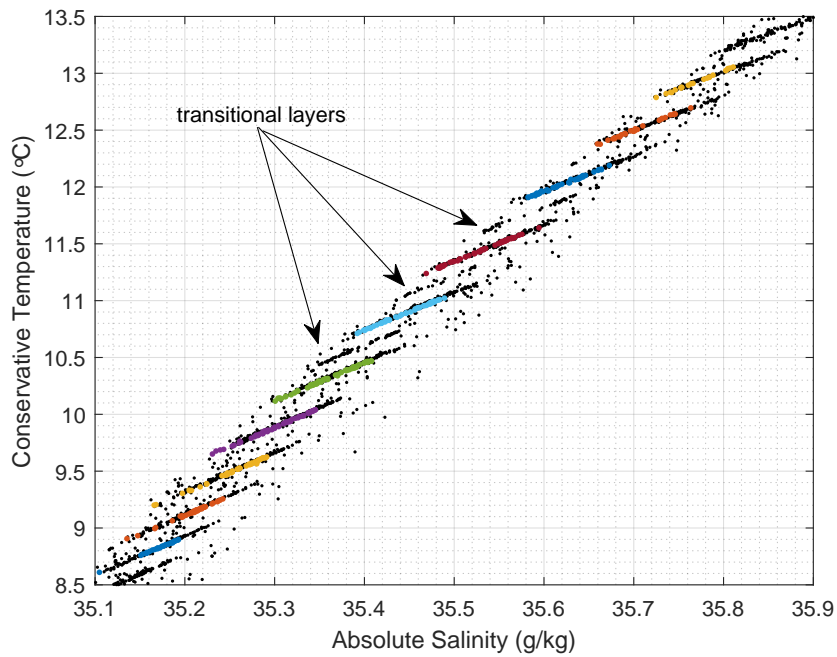


Figure 5: Absolute Salinity (g/kg) and Conservative Temperature ($^{\circ}C$) of all detected homogeneous layers, indicated by dots. Black dots for all detected homogeneous layers. Transitional layers are indicated by arrows. For later reference, 10 lines are distinguished by a unique colour code representing detected homogeneous layers from Argo float 3901979. The same colour code is used in Figures 6, 8 and 10.

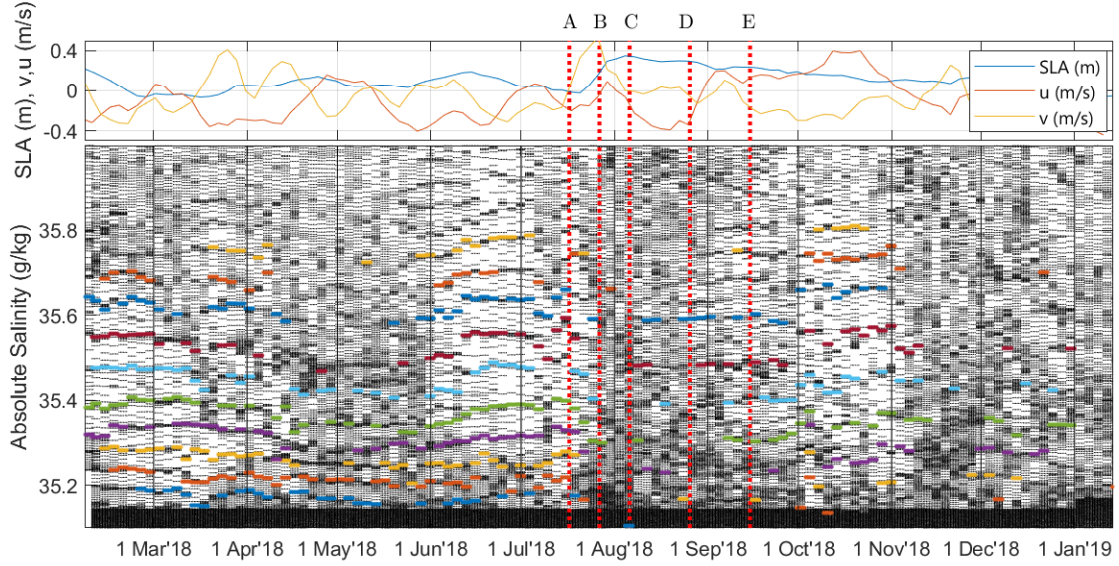


Figure 6: (a) sea level anomaly (m) and geostrophic velocities (m/s) at the profile location. (b) absolute Salinity sampled by float 3901979 over the period 06/Feb/2018 to 13/Jan/2019 in depth interval 100 – 2000 $dbar$. Every dot corresponds to 1 depth measurement taken with an interval of 1 $dbar$. A tight grouping of points represents a homogeneous layer and white patches indicate an interface, the sequence of both indicates a step. Coloured dots are plotted at detected homogeneous layers related through the flux ratio ($\gamma = \alpha F_T / \beta F_S$). The colour code is similar to Figures 5, 8 and 10. Vertical dotted red lines with A-E on top indicate moments in time at which snapshots of the sea surface anomaly are represented in Figure 7.

flux which gives the strong indication that the change in properties of a staircase is caused by double diffusive mixing (Radko, 2013). We found no significant long term or spatial pattern giving the indication that the temperature and salinity variation of staircases is governed by short term processes. We furthermore found that profiles with well-developed steps are on average warmer and more saline than profiles with an absence of steps (compare Figure 3a and d). Well-developed steps are thus likely represented by the top right corner of the lines in Figure 5. Our data thus gives the strong indication that staircases in the Caribbean Sea can be represented by an average staircase profile of relatively warm and saline well developed steps and that a deviation in step type, likely determined by short term processes, is accompanied by a decrease in temperature and salinity, indicating a horizontal or vertical double diffusively induced flux divergence. This argument is further explored in the case study of Chapter 4.

4 Case study: anticyclonic eddy

In the previous section we argued that the variation in step types and the variation in temperature and salinity of steps is likely related to short term processes. Staircases measured by float 3901979 (purple line in Fig. 1) showed a significantly lower temperature and salinity from the end of July 2018 to the end of October 2018, relative to temperature and salinity of staircases in the previous months, coinciding with a decrease in the number of well-defined steps. This event coincided with an anticyclonic eddy which we will study in this section.

In Figure 6b a sequence of white patches and a dense packing of points represents a step (as seen from 1/Jun/2018 till 1/Jul/2018). A relatively homogeneous vertical distribution of dots indicates an absence of steps (as seen from 1/Aug/2018 till 1/Sep/2018). Homogeneous layers related in temperature and salinity by the flux ratio ($\gamma = \alpha F_T / \beta F_S$) are indicated by dots of the same colour (same colour code as in Fig. 5). Figure 6b shows that in regions with well-developed steps (Fig 3a) the salinity is relatively high (as seen from 1/Jun/2018 to 1/Jul/2018) as also indicated in Chapter 3.2. In time intervals with less well-defined steps the salinity of steps is relatively low (as seen from 1/Aug/2018 to 1/Sep/2018).

In Figure 6 ten steps are distinguished, each with a different colour code. All steps show a relatively low/high salinity in the same periods but steps higher in the water column (higher salinity in Fig. 6b) tend to show a larger variation in salinity than steps lower in the water column. The steps in the middle of the water column ($S = 35.3 - 35.6 \text{ g/kg}$ in Fig. 6b) are most often observed in vertical salinity profiles.

4.1 Eddy characteristics

Snapshots of the sea level anomaly are shown in Figure 7. In this period the float first travelled through a region with a negative sea level anomaly (period A-B in Fig. 7), after which it travelled through a strong anticyclonic eddy (period B-D in Fig. 7) until the anticyclonic eddy splits (D and E in Fig. 7). The diameter of the anticyclonic eddy is approximately 500 km and geostrophic velocities exceed 0.5 m/s (CMEMS).

The Argo floats do not store data on the vertical velocity structure. The vertical structure of the eddy in this case study is thus unknown. The eddy can have two vertical structures; 1) if the eddy azimuthal velocity is significantly high at the the staircase depth, the eddy may be viewed as a lense of water travelling through the Caribbean Sea and advecting the staircases in the eddy interior. Staircases at the eddy edge are then also affected by significant vertical shear. 2) if the eddy azimuthal velocity is relatively low at the staircase depth range, the staircases are only slightly affected by vertical shear. Staircases are, however, affected by eddy induced lateral temperature and salinity gradients.

4.2 Observations

In this section we present our observations of the staircases in relation to the anticyclonic eddy. In the subsequent sections the observations are placed in perspective. We note that our data should

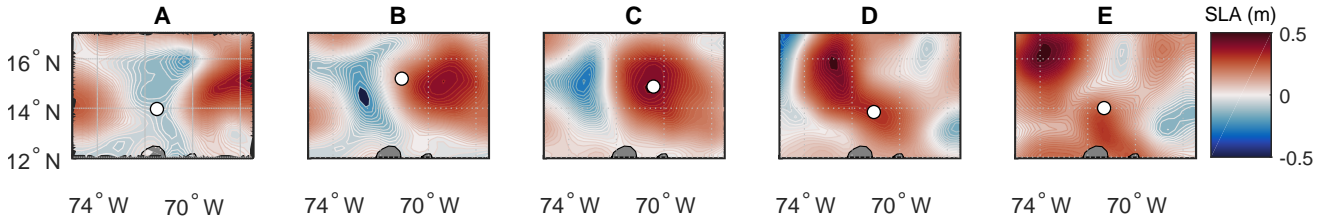


Figure 7: Sea level anomaly (m) and float location (white dot) at five different moments in time; A: 17/Jul/2018 B: 27/Jul/2018 C: 6/Aug/2018 D: 26/Aug/2018 E: 15/Sep/2018. The grey areas at $12^\circ N$ represent the northern coasts of South-America. The domains of the sub-figures are the same. (Colourmap from Thyng et al., 2016).

be interpreted as semi Lagrangian (see section 2.2) and any development that we will describe in the following paragraphs is not necessarily a development in time or space, but solely a discussion of the developments we observe in the vertical profiles taken with a 3 day time interval by float 3901979.

We will discuss the vertical temperature profiles in Figure 8b in relation to the float position in time, shown in Figure 7. In Figure 8 we observe well-developed steps before 1/Jul/2018, which is before the float enters the area of a negative sea level anomaly shown in Figure 7. Just before the float arrives at position (A) in Figure 7 we observe well-defined steps, transitional layers and intrusions (from 1/Jul/2018 to point A in Figure 8b). From points A to B in Figures 7 and 8b, and thus in an area of strong lateral sea surface gradients, we observe a few well-developed steps, transitional layers but mostly an absence of staircases. From B to C in Figures 7 and 8b, and thus under the core of the eddy, we observe an absence of staircases. From points C to E in Figures 7 and 8b we see that the float leaves the eddy core which coincides with observations of transitional layers, inversions and, at the end of the period, well-developed layers.

We will now discuss the change in properties of a single step. This step is identified in different vertical temperature profiles as the temperature and salinity of the homogeneous layer change with the flux ratio (γ). We will discuss the step identified by the green line in Figures 5, 6b and 8b as this layer is most often observed in the vertical temperature profiles. In Figure 8c the pressure level of this step is plotted. The increase in pressure of this step coincides with an increase in sea surface anomaly as found by comparing for example the pressure level at point B in Figure 8c with the sea surface anomaly at point B in Figures 8a and 7). This may indicate that steps are pushed down because of the positive sea surface anomaly at the eddy core.

In Figure 8d the temperature and salinity of the green step are shown. An increase in pressure (for example from point A to B in Figure 8c) coincides with a decrease in temperature and salinity of the step (point A to B in Figure 8d). Temperature and salinity of staircases are related through the flux ratio ($\gamma < 1$) and with the salt flux exceeding the heat flux we also observe a decrease in the potential density anomaly (kg/m^3) coinciding with a decrease in temperature and salinity

(point A to B, in Figure 8d and c, green line).

Figures 6b and 10 show that the observations made for one step apply to the whole layer. For example, in Figure 10 we see that all steps (indicated by coloured dots) reside at a higher salinity and lower pressure at time B (eddy edge, see Fig. 7B) compared to time C (eddy core, see Fig. 7B).

To conclude, we see that the staircase types are likely related to the temperature and salinity. Well-developed steps have a higher temperature and salinity than the occasional step in a profile largely of type IV. Vertical profiles of types II and III have steps with an intermediate temperature and salinity.

4.3 Influence of eddy induced shear

In section 3.1 we linked types II (transitional layers) and IV (absence of staircases) to the presence of shear. We argued that turbulence likely leads to an increased high gradient layer thickness possibly ultimately resulting in a transitional layer. Our observations show that transitional layers are present at the edge of the anticyclonic eddy where the azimuthal velocity and thus shear induced turbulence, is likely high (around times B and D,E in Figures 7 and 8b).

In section 3.1 we argued that an absence of staircases in a depth range with $1 < R_\rho < 2$ is usually associated with a high energy environment (Radko, 2013). Turbulent mixing can destroy staircases if turbulent mixing is higher than finger driven mixing (St. Laurent and Schmitt, 1999; Radko, 2013). Type IV profiles are, however, observed under the eddy core (C in Fig. 8) where the eddy azimuthal velocity, and shear induced turbulence, is likely low. Another reason for an absence of staircases in the core might be that staircases were never formed in the eddy interior, which may be the case if the water mass in which staircases are residing is trapped in the eddy interior (see the discussion on eddy types in section 4.2). The lack in formation may be due to weak lateral isohaline gradients in the eddy interior (Merryfield, 2000). However, if the staircases are not trapped inside the eddy they may still be destroyed at the eddy edges by a strong, eddy induced, vertical shear. Subsequent formation may slow or absent, possibly due to weak lateral isohaline gradients under the eddy core (Merryfield, 2000). If the vertical temperature profiles show this process of destruction and slow formation we may hypothesize that this process follows a sequence starting with well-developed staircases (possibly representing an equilibrium profile), followed by profiles with transitional layers and intrusions and ending in profiles with an absence of staircases. We can, however, not give a definite conclusion because the data interpretation is far from straightforward (see section 2.2).

4.4 Influence of eddy induced lateral isohaline gradients

An anticyclonic eddy is characterised by a warm core and an increased water level. As a result, isohalines under the eddy core are located lower in the water column with respect to the eddy exterior. Lateral gradients in isohalines may lead to thermohaline intrusions (see discussions in Ruddick and Richards, 2003a,b; Radko, 2013). Our data suggests that in the anticyclonic eddy of our case study, isohalines are also displaced downward under the eddy core (see time C in Fig.

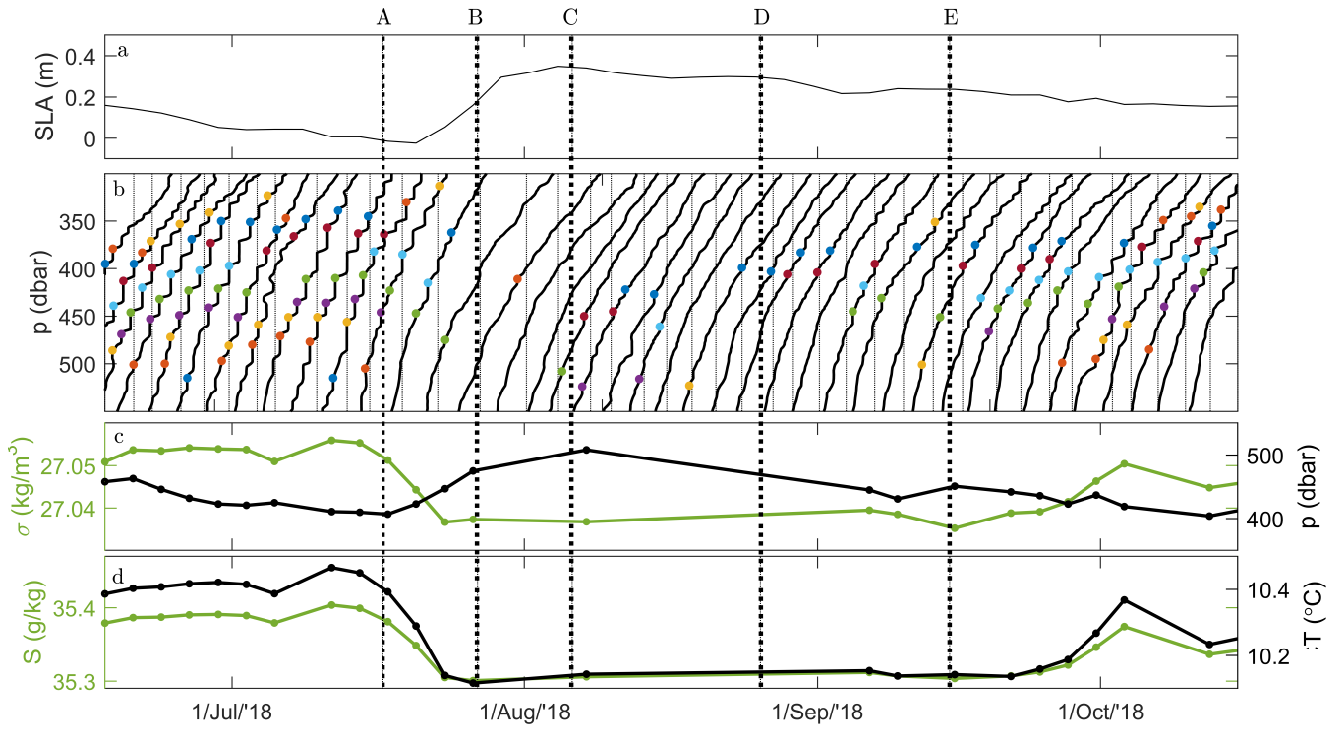


Figure 8: (a) sea level anomaly (m) at the float's location over the period from 17/June/2018 till 15/October/2018. (b) vertical temperature profiles with steps related through the flux ratio indicated by dots of the same colour over the period from 17/June/2018 till 15/October/2018. Profiles are shown with an arbitrary offset and a 3 day time interval. Thin dashed vertical lines indicate the moment in time of a vertical profile and intersect the vertical temperature profiles at 400 dbar. (c) potential density (green line, left axis) and pressure (black line, right axis) of the step indicated by a green dot in (b) over the period from 17/June/2018 till 15/October/2018. (d) Absolute Salinity (green line, left axis) and Conservative Temperature (black line, right axis) over the period from 17/June/2018 till 15/October/2018. Vertical dotted lines and letters A-E on top of (a) indicate moments in time of which screenshots of the sea level anomaly are shown in Figure 7.

10).

In Figure 9 a schematization of thermohaline intrusions is shown (Ruddick and Richards, 2003b). The grey arrow starting at A is an intrusion advecting relatively cold and fresh water (lower left corner) to a warm and salty environment (upper right corner). The intrusion ending at B advects relatively warm and salty water to a cold and fresh environment. Vertically cold and fresh intrusions are interchanged by warm and salty intrusions. This sequence results in an increased temperature and salinity gradient in regions under warm and salty intrusions and a decreased temperature and salinity gradient in regions above warm and salty intrusions. An increased temperature and salinity gradient results in an increased salt finger temperature and salinity flux (Ruddick and Richards, 2003b), and vice versa for a weakened gradient, which implies a flux convergence at cold and fresh, downward moving, intrusions and a flux divergence for warm and salty, upward moving, intrusions. We found a flux ratio of $\gamma = 0.79$ which thus exceeds the heat flux, and thus implies an increased density for cold and fresh, downward moving, intrusions which amplifies the initial movement. Warm and salty intrusions thus become less dense which also amplifies the initial movement (Ruddick and Richards, 2003b).

Since our data gives the strong indication that isohalines are displaced downward under the core of the eddy of our case study (Fig. 10), we may apply Figure 9 to our data. Following the schematisation of Figure 9, cold and fresh intrusions are directed from the eddy exterior to the eddy core. Warm and salty intrusions are directed from the eddy core towards the eddy exterior. Temperature and salinity of the staircases are lower under the eddy core with respect to the eddy exterior (see section 4.2) and thermohaline intrusions may cause this variation because (1) the variation is with the flux ratio (γ) which thus implies a flux divergence due to thermohaline processes, and (2) warm and salty intrusions are directed to the eddy exterior while cold and fresh intrusions are directed towards the eddy interior corresponding to the relatively low temperature and salinity of steps we observed under the eddy core (Fig. 6 and 8d).

If the staircases are advected with the eddy (see section 4.1) the horizontal intrusions are likely causing a constant diapycnal buoyancy flux at the eddy front. If the staircases are not advected with the eddy we should interpret the intrusions as an instantaneous effect. The eddy displaces isohalines resulting in local intrusions. In both cases the eddy preconditions water masses such that thermohaline intrusions can develop. This gives the strong impressions that the eddy is a catalyst in double diffusive transport.

5 Discussion

Our aims were to provide a general overview of thermohaline staircases in the Caribbean Sea and to investigate the influence of eddies on staircases. We analysed 460 vertical temperature and salinity profiles of staircases which is a significant increase of the available data compared to a previous total of 53 vertical profiles (Lambert and Sturges, 1977; Morell et al., 2006; van der Boog et al., 2019). The interpretation of our dataset was however not straightforward because, due to the relatively low flow velocities at parking depth, the Argo floats were partly advected with the staircase layer but also partly advected at the surface. In a future study we therefore suggest to pay attention to this difference in flow velocities and to make sure that the data is either Eulerian

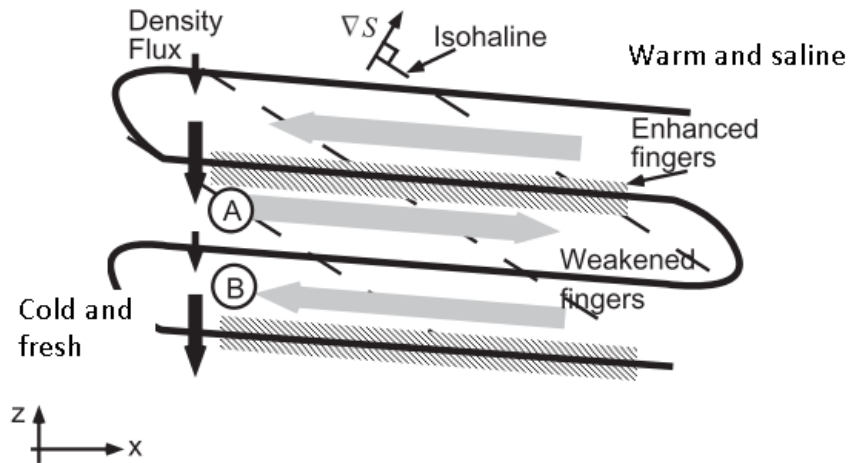


Figure 9: Schematic of the mechanism of intrusions growth in the salt finger regime. Warm and saline water in the top right corner, cold and fresh water in the lower left corner. Isohalines are indicated with striped lines, intrusions are indicated with arrows. Intrusions result in a pattern of increased and decreased vertical buoyancy flux as indicated by the relative size of the black arrows. (figure from: Ruddick and Richards (2003b)).

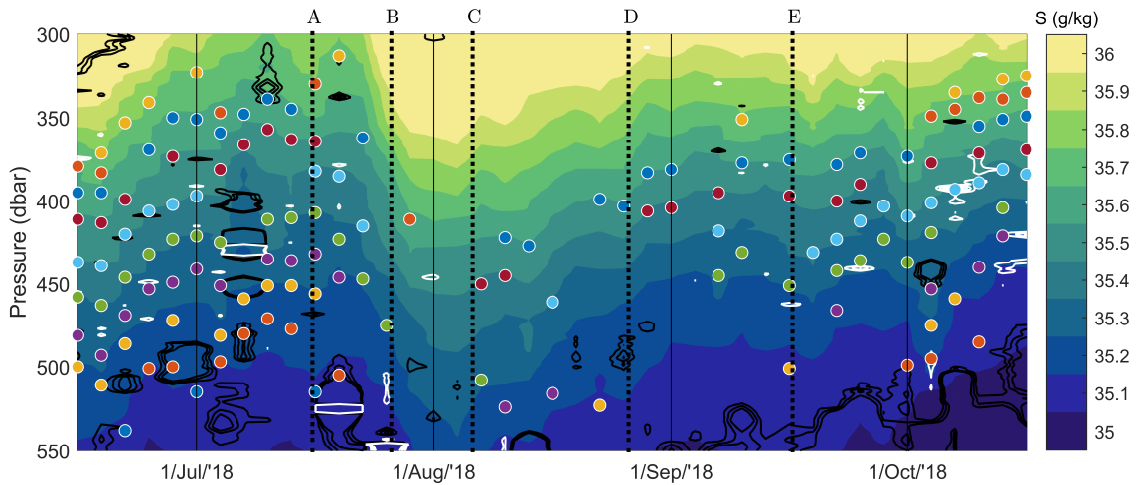


Figure 10: Absolute salinity (g/kg) in the interval $35 : 0.1 : 36 g/kg$ measured by Argo float 3901979 over the period 17/Jun/2018 till 15/Oct/2018. Black contour lines indicate anomalously high values of the density ratio at intervals $R\rho = 1.9 : 0.1 : 2.1$ and white contour lines indicate anomalously low values of the density ratio at intervals $R\rho = 1 : 0.1 : 1.4$. Coloured dots indicate steps related through the flux ratio (γ) of which the colour code is similar to Figures 5, 6 and 8. Thin black vertical lines at 1/Jun/2018, 1/Aug/2018, 1/Sep/2018 and 1/Oct/2018. Thick dotted lines with A-E on top indicate moments in time at which snapshots of the sea surface anomaly are presented in Figure 7. Colourmap from Thyng et al. (2016).

or Lagrangian.

We hypothesised that the Caribbean Sea equilibrium staircase profile is relatively warm and saline with well-developed steps. We, however, also observed an absence of staircases. We related the absence to the presence of a strong anticyclonic eddy. An absence of staircases was observed under the eddy core which is in contrast to the findings of van der Boog et al. (2019) who found no difference in staircase types related to the presence of an anticyclonic eddy. The eddy in van der Boog et al. (2019) was with a diameter of 180 *km* however much weaker than the anticyclonic eddy in our case study with a diameter of 500 *km*. The eddy in our study may thus have extended further downward thereby affecting the staircases. We, however, do not have information to substantiate this argument and suggest a future study including velocity measurements.

Morell et al. (2006) investigated staircases under a cyclonic eddy and found an absence of staircases under the eddy core which might be related to change in the background gradients as in the eddy core relatively cold and fresh waters are located. Vertical temperature and salinity gradients are thus lower compared to the background state with relatively warm and saline surface waters. A decrease in vertical gradients affects the density ratio ($R_\rho = \alpha \bar{T}_z / \beta \bar{S}_z$) which should be in a critical range to observe staircases (St. Laurent and Schmitt, 1999). In our study we, however, found that the absence of staircases is not related to the density ratio. We therefore hypothesize that the absence of staircases in our study may be related to a lack of formation. Either after previous destruction or due to the absence of lateral gradients in the eddy core (Merryfield, 2000). We should however verify this with more data and possibly a modelling orientated study.

We linked staircases through temperature and salinity changing with a constant flux ratio ($\gamma = \alpha F_T / \beta F_S$) and subsequently found that individual layers have a lower temperature and salinity under the eddy core with respect to the eddy exterior, as also found in Marmorino (1991). Schmitt et al. (1987) found a northward increase in temperature and salinity with a similar flux ratio and attributed this effect to a conversion of water mass properties. We found no statistical evidence for the findings of Schmitt et al. (1987) but it may well be that the anticyclonic eddy we studies advected a relatively cold and fresh water mass. A northward increase in temperature and salinity in the Caribbean Sea may also be overshadowed by the effect of eddies. We observed a lower temperature and salinity at time periods other than the case study but we were not able to identify the cause, possibly because the effect was weaker than the strong anticyclonic eddy in the case study. A future investigation of these other time periods may give a more comprehensive view of the cause of the temperature and salinity variation of staircases in the Caribbean Sea.

To quantify a vertical double diffusive flux, often a so-called '4/3 flux law parametrisation' (Turner, 1967) is used. We used form of Schmitt (1979) in Bebieva and Timmermans (2016):

$$F_T = C \frac{\gamma \rho c_p}{\alpha} (g \kappa)^{1/3} (\beta \Delta S)^{4/3} \quad (6)$$

In which $C = 0.05 + 0.3 R_\rho^{-3} = 0.088$ is an empirical function of the density ratio, ΔS is the salinity jump across an interface, $\gamma = \alpha F_T / \beta F_S = 0.79$ is the flux ratio, $c_p = 3980 J / (kg^\circ C)$ is the specific heat of seawater, $\rho = 1025 kg/m^3$ is the approximate density of TACW, $\kappa = 1.4 \times 10^{-7} m^2 s^{-1}$ is the molecular diffusivity of heat and $g = 9.81 ms^{-2}$ is the gravitational acceleration. We used $\Delta S = 0.8 g/kg$ to get $F_T = -70 W/m^2$ and, using the flux ratio, $F_S = -5 \times 10^{-6} m/s$. We estimate the diffusivity of heat (K_T) and the diffusivity of salt (K_S) from:

$$F_T = \rho c_p K_T \bar{T}_z \quad (7)$$

$$F_S = K_S \bar{S}_z \quad (8)$$

$\bar{T}_z = -0.03 \text{ }^\circ\text{C}/\text{dbar}$ is the approximate background temperature gradient and $\bar{S}_z = -0.006 \text{ (g/kg)}/\text{dbar}$ is the approximate background salinity gradient. We thus calculated $K_T = 3.5 \times 10^{-4} \text{ m}^2/\text{s}$ and $K_S = 9 \times 10^{-4} \text{ m}^2/\text{s}$. These values are an order of magnitude higher than $K_T = 0.45 \times 10^{-4} \text{ m}^2/\text{s}$ and $K_S = 0.9 \times 10^{-4} \text{ m}^2/\text{s}$ obtained through a tracer release experiment (Schmitt et al., 2005). Kunze (2003) argued that laboratory flux laws are known to overestimate oceanic double diffusive fluxes because the interface of oceanic staircases is thicker than the interface in laboratory staircases. A thicker interface implies less strong vertical gradients and thus a lower flux (Kunze, 2003). Thicker interfaces may formed due to shear (Radko, 2013). We observed thicker interface under the eddy edge possibly substantiating this argument.

In conclusion, our investigation gave the strong indication that, despite the occasional observations of an absence of steps, staircases in the Caribbean Sea are generally constant in time and space. Despite a lack of quantification of the vertical temperature and salinity flux, we know from earlier studies that staircases are very effective in diapycnal transport (Schmitt et al., 2005; Radko, 2013) and we may thus hypothesise that staircases in the Caribbean Sea provide a constant and effective diapycnal mixing, likely increased due to the preconditioning of water masses by strong Caribbean eddies.

References

- Bebieva, Y. and Timmermans, M. L. (2016). An examination of double-diffusive processes in a mesoscale eddy in the Arctic Ocean. *Journal of Geophysical Research: Oceans*, 121(1):457–475.
- Biescas, B., Armi, L., Sallarès, V., and Gràcia, E. (2010). Seismic imaging of staircase layers below the Mediterranean Undercurrent. *Deep-Sea Research Part I: Oceanographic Research Papers*, 57(10):1345–1353.
- Durante, S., Schroeder, K., Mazzei, L., Pierini, S., Borghini, M., and Sparnocchia, S. (2019). Permanent Thermohaline Staircases in the Tyrrhenian Sea. *Geophysical Research Letters*, 46:1562–1570.
- Fer, I., Nandi, P., Holbrook, W. S., Schmitt, R. W., and Páramo, P. (2010). Seismic imaging of a Thermohaline Staircase in the Western Tropical North Atlantic. *Ocean Science*, 6(3):621–631.
- Gordon, A. L. (1967). Circulation of the Caribbean Sea. *Journal of Geophysical Research*, 72(24):6207–6223.
- Kunze, E. (2003). A review of oceanic salt-fingering theory. *Progress in Oceanography*, 56:399–417.
- Lambert, R. B. and Sturges, W. (1977). A thermohaline staircase and vertical mixing in the thermocline. *Deep-Sea Research*, 24:211–222.

- Marmorino, G. O. (1989). Substructure of oceanic salt finger interfaces. *Journal of Geophysical Research*, 94(C4):4891–4904.
- Marmorino, G. O. (1991). Intrusions and diffusive interfaces in a salt-finger staircase. *Deep-Sea Research*, 38(11):1431–1454.
- McDougall, T. J. and Barker, P. (2011). Getting started with TEOS-10 and the Gibbs Seawater (GSW) Oceanographic Toolbox. 28pp., *Scor/Iapso Wg127*, ISBN 978-0-646-55621-5.
- Merryfield, W. J. (2000). Origin of Thermohaline Staircases. *Journal of Physical Oceanography*, 30(5):1046–1068.
- Morell, J. M., Corredor, J. E., and Merryfield, W. J. (2006). Thermohaline staircases in a Caribbean eddy and mechanisms for staircase formation. *Deep-Sea Research Part II: Topical Studies in Oceanography*, 53:128–139.
- Radko, T. (2003). A mechanism for layer formation in a double-diffusive fluid. *Journal of Fluid Mechanics*, 497:365–380.
- Radko, T. (2005). What determines the thickness of layers in a thermohaline staircase? *Journal of Fluid Mechanics*, 523:79–98.
- Radko, T. (2013). *Double-diffusive convection*. 344pp., Cambridge University Press, N.Y.
- Ruddick, B. and Hebert, D. (1988). The Mixing of Meddy Sharon. *Elsevier Oceanography Series*, 46(C):249–261.
- Ruddick, B. and Richards, K. (2003a). Oceanic thermohaline intrusions: observations. *Progress in Oceanography*, 56:499–527.
- Ruddick, B. and Richards, K. (2003b). Oceanic thermohaline intrusions: theory. *Progress in Oceanography*, 56:483–497.
- Schmitt, R. W., Ledwell, J. R., Montgomery, E. T., Polzin, K. L., and Toole, J. M. (2005). Ocean science: Enhanced diapycnal mixing by salt fingers in the thermocline of the tropical atlantic. *Science*, 308:685–688.
- Schmitt, R. W., Perkins, H., Boyd, J., and Stalcup, M. (1987). C-SALT [Caribbean-Sheets and Layers Transects]: an investigation of the thermohaline staircase in the western tropical North Atlantic. *Deep Sea Research*, 34(10):1655–1665.
- St. Laurent, L. and Schmitt, R. W. (1999). The Contribution of Salt Fingers to Vertical Mixing in the North Atlantic Tracer Release Experiment. *Journal of Physical Oceanography*, 29(7):1404–1424.
- Thyng, K. M., Greene, C. A., Hetland, R. D., Zimmerle, H. M., and DiMarco, S. (2016). True colors of oceanography: Guidelines for effective and accurate colormap selection. *Oceanography*, 29(3):9–13.

- Turner, J. (1967). Salt fingers across a density interface. *Deep-Sea Research*, 14:599–611.
- van der Boog, C. G., de Jong, M. F., Scheidat, M., Leopold, M. F., Geelhoed, S. C. V., Schulz, K., Dijkstra, H. A., Pietrzak, J. D., and Katsman, C. A. (2019). Hydrographic and Biological Survey of a Surface-Intensified Anticyclonic Eddy in the Caribbean. Confidential manuscript submitted for publication to *Journal of Geophysical Research: Oceans*.
- Zodiatis, G. and Gasparini, G. P. (1996). Thermohaline staircase formations in the Tyrrhenian Sea. *Deep-Sea Research Part I: Oceanographic Research Papers*, 43(5):655–678.